crystals

MDPI

Article

Performance Investigation of the Incorporation of Ground Granulated Blast Furnace Slag with Fly Ash in Autoclaved Aerated Concrete

Vijay Antony Raj Bernard [1], Senthil Muthalvan Renuka [1], Siva Avudaiappan [2,3,*], Chockkalingam Umarani [1], Mugahed Amran [4,5,*], Pablo Guindos [3], Roman Fediuk [6,7] and Nikolai Ivanovich Vatin [6]

1 Department of Civil Engineering, College of Engineering Guindy, Anna University, Chennai 600025, India; bvijayantonyraj@gmail.com (V.A.R.B.); renuka@annauniv.edu (S.M.R.); umarani@annauniv.edu (C.U.)
2 Departamento de Ingeniería Civil, Universidad de Concepción, Concepción 4030000, Chile
3 Centro Nacional de Excelencia para la Industria de la Madera (CENAMAD), Pontificia Universidad Católica de Chile, Av. Vicuña Mackenna 4860, Santiago 8330024, Chile; pguindos@uc.cl
4 Department of Civil Engineering, College of Engineering, Prince Sattam Bin Abdulaziz University, Alkharj 16273, Saudi Arabia
5 Department of Civil Engineering, Faculty of Engineering and IT, Amran University, Amran 9677, Yemen
6 Polytechnic Institute, Far Eastern Federal University, 690922 Vladivostok, Russia; fedyuk.rs@dvfu.ru (R.F.); vatin@mail.ru (N.I.V.)
7 Peter the Great St. Petersburg Polytechnic University, 195251 St. Petersburg, Russia
* Correspondence: savudaiappan@udec.cl (S.A.); m.amran@psau.edu.sa (M.A.)

Abstract: Autoclaved aerated concrete (AAC) is one of the most common types of lightweight cellular concrete, having a density of approximately one-fourth of that of conventional plain cement concrete. The use of industrial waste materials in concrete as a replacement for cement has garnered a lot of attention in recent years as a way to reduce the environmental effect of concrete. In this study, an attempt has been made to study the effect of AAC blocks made of industrial wastes such as fly Ash (FA) and ground granulated blast furnace slag (GGBS). Fly ash, along with different dosages of GGBS, was used as a partial replacement for cement in the production of AAC. For all the different dosages, microstructural analysis was performed using a Scanning electron microscope (SEM), X-ray diffraction (XRD), energy dispersive X-ray spectroscopy (EDAX), and Fourier transform infrared spectroscopy (FTIR). Mechanical performances of AAC were determined by conducting various tests like compressive strength, modulus of rupture, dry density, and water absorption. The results revealed that the dosage of "15% GGBS + 85% cement" has maximum compressive strength, modulus of elasticity, and modulus of rupture made of Class F Fly Ash when compared to Class C Fly Ash based AAC blocks. Besides, the incorporation of GGBS in the manufacturing process would increase the compressive strength of AAC up to 68%. Hence, it is recommended to use 15% GGBS + 85% cement as a potential rate of replacement, to improve the mechanical properties of AAC blocks significantly.

Keywords: autoclaved aerated concrete; fly ash; GGBS; mechanical properties

Citation: Bernard, V.A.R.; Renuka, S.M.; Avudaiappan, S.; Umarani, C.; Amran, M.; Guindos, P.; Fediuk, R.; Ivanovich Vatin, N. Performance Investigation of the Incorporation of Ground Granulated Blast Furnace Slag with Fly Ash in Autoclaved Aerated Concrete. *Crystals* **2022**, *12*, 1024. https://doi.org/10.3390/cryst12081024

Academic Editors: José L. García and Pavel Lukáč

Received: 28 June 2022
Accepted: 20 July 2022
Published: 23 July 2022

1. Introduction

Autoclaved aerated concrete (AAC) was first attempted to produce in 1889 by Czechoslovakian researcher Hoffman [1]. In 1914, Aylsworth and Dyer [2] incorporated aluminum powder and calcium hydroxide as agents to form a cementitious matrix in AAC [3]. Later in 1919, German researcher, Grosahe used metal powder as hydrogen gas to form AAC [3]. Several attempts were carried out during the 1880s to 1920s to produce lightweight AAC. Finally, Swedish researcher Johan Axel Eriksson in 1923 found the perfect mix for the manufacturing of AAC [4,5]. Several investigations have been performed on the development of AAC with different byproducts [6–8]. The physical, chemical, mechanical, and functional

characteristics were investigated as per the testing and design by RILEM recommended practices [9].

The AAC is the most widely used lightweight construction material that is commonly employed in the form of blocks [7]. Because of the high porosity, the houses have a low density and excellent insulation. The low density is achieved by forming air spaces to give a cellular structure [10]. The finished result is up to five times the volume of the raw materials used, with an air content of 70–80%, relying on the needed power and density that may be preserved, fastened, and drilled without issues even more than lumber [11]. The AAC is a lightweight concrete block with a density ranging from 300–1800 kg/m^3. In high-rise building construction, lightweight concrete block is widely used to reduce the dead weight of the structure and thereby, less weight will be transferred to the foundation [12]. The ingredients of AAC are cement, fly ash or sand, lime powder, gypsum, soap oil, water, and aluminum powder in a range of 0.04–0.05% in volume of the concrete [13]. The aluminum powder plays an important role in aerating the entire concrete matrix and creates a cellular structure that occurs in the cementitious phase [14]. In the cementitious phase, calcium silicate hydrate gels and hydrogen gas help to double the volume of concrete [15–17]. The entire process of the cementitious phase to form a concrete matrix is around 30–45 min. During this, aerated concrete produces tobermorite in the pre-curing stage. In the transition reactional phase, the tobermorite $\{Ca_5\ [Si_6\ O_{16}\ (OH)_2].\ 2H_2O\}$ changes into xonotlite $\{C_6S_6O_{17}\ (OH)_2\}$ [18–20].

Muthu et al. [21] experimented with the effect of fineness and dosages of aluminum powder on the properties of AAC. The property of the concrete medium was evaluated based on the workability variations, aeration rate, fresh density, dry density, compressive strength, and percentage of water absorption. It was reported that the strength to density ratio of the aerated concrete is purely dependent on the fineness of the aluminum powder and its dosage; in addition, the water–cement ratio plays a major role in determining the strength of the aerated concrete. Onur et al. [22] determined the effect of polypropylene fibers in AAC, through which an increase in compressive strength, bending strength, and thermal conductivity of the concrete has been observed as the length of the fiber in the concrete mix increases. Rafiza et al. [23] used recycled AAC as a replacement for sand in a new type of AAC to determine its mechanical properties. The experimental results confirmed an increase in strength of about 16% compared to conventional AAC. Pawel et al. [24] investigated the performance of fly ash-based AAC with a density in the range of 350 kg/m^3. The performance of both sand-based AAC and fly ash-based AAC was compared. It was concluded that fly ash-based AAC possesses better thermal insulation and less product of hydration when compared with that of sand-based AAC. Kittipong et al. [25] investigated the influence of replacing black rice husk ash and bagasse ash in AAC under different temperatures. It is reported that unburned carbon and alkaline ashes can be used as raw material in AAC. Additional strength gain is achieved because of the formation of tobermorite through katoite; also, in addition, the presence of other alkalis from the residues enables to stabilize tobermorite in plate form.

Yang et al. [26] autoclave aerated concrete waste effectively refines the pore structure and improves the micro-hardness of the interfacial transition zone (ITZ) through internal curing, and enhances the resistance to chloride penetration. Peng et al. [27] produce AAC by using graphite tailings as siliceous material. The results manifested that, except for the cement dosage, water-solid materials ratio, and foaming agent content, the calcium-silicon ratio also plays an important role in the production of Graphite Tailings-AAC. The usage of industrial wastes/by-products like the utilization of coal bottom ash, copper tailings, waste perlite, iron tailings, and coal gangue were reported in the past five years [28–32].

Several investigations have shown that ground granulated blast furnace slag (GGBS) improves the mechanical characteristics of concrete significantly [33–38]. GGBS improved the compressive strength of AAC blocks by 172% [39]. In the same investigation, replacing 21% of the cement with weight boosted tensile strength by 25% [11]. The inclusion of GGBS reduced water absorption by 45%. Along with silica fume, GGBS and zeolite were

investigated in the study by Pachideh et al. [39]. Both increased the characteristics of AAC blocks in the same way that GGBS did. Among the three pozzolonas [40–42], silica fume [43–46] was more efficient than the others in increasing strength and decreasing water absorption.

However, there has been little research on the influence of GGBS and fly ash on aerated concrete; thus, more research is required [11,47]. Thus, the investigation on finding which class of fly ash, either class C or class F is suitable for AAC has not been done so far. Hence, in this experimental work using, both classes of fly ash were used for the production of AAC along with its strength and microstructural studies. Microstructural studies like SEM and XRD were conducted in previous studies [7,18]; these investigations will be helpful for finding the pore formation and structure of AAC. From the literature, it is observed that the utilization of industrial wastes and by-products improves the performance of AAC on the basis of economy and durability parameters.

2. Materials

2.1. Cement

In this study, Ordinary Portland Cement of 53 grades was used. Cement confirming to IS: 12269:2013 [48] and IS: 4031:1988 [49] was followed to perform basic tests on cement. The quantity of cement used in this investigation was 18% of the volume in aerated concrete. Figure 1a,b clearly shows the SEM and EDAX image of OPC 53 grade of cement.

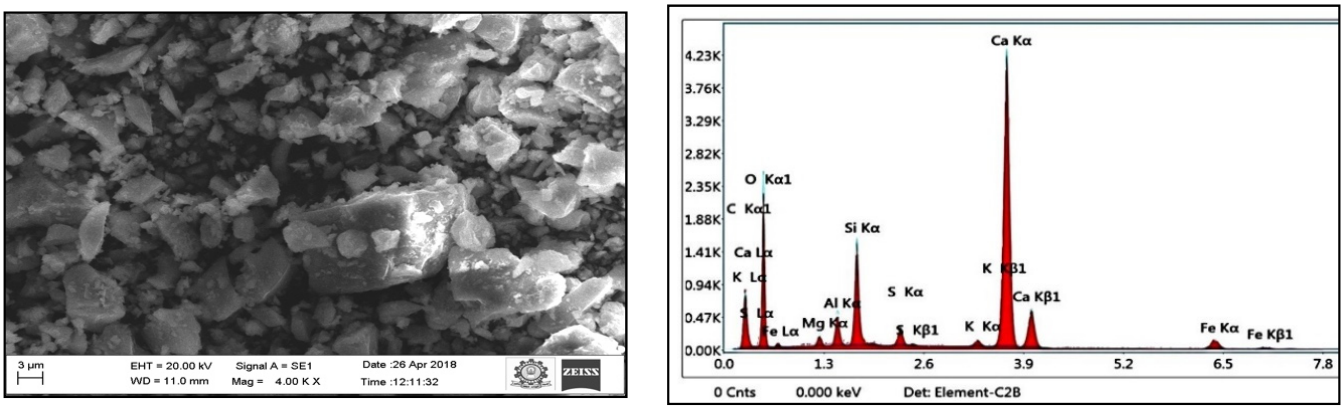

(**a**) (**b**)

Figure 1. (**a**) SEM image of OPC 53 grade cement; (**b**) EDAX image of OPC 53 grade cement.

2.2. Fly Ash

Class C fly ash was obtained from Ennore thermal power plant and Class F was brought from Neyveli Lignite Corporation for this investigation. The bulk density and the fineness of these two different fly ashes were found to have closer values, whereas the specific gravity of Class C fly ash was around 2.6 and for Class F fly ash, it was around 1.94. In the chemical composition, Class C Fly ash contains SiO_2 around 35% to 40%, Fe_2O_3, Al_2O_3, CaO, and SO_3 each in the range of 10% to 15%, whereas Class F Fly ash contains a high concentration of SiO_3, which is around 55% to 60% and Al_2O_3 in the range of 25% to 30%. Fly ash acts as a binder and filler material in aerated concrete as well as contributing to the secondary hydration process. The volume of fly ash was 54% in the entire aerated concrete [50]. Figure 2a,b clearly shows the SEM and EDAX image of Class C fly ash and Figure 3a,b clearly shows the SEM and EDAX image of Class F fly ash and Table 1 shows the Physical and Chemical compositions of Cement, FA, and GGBS.

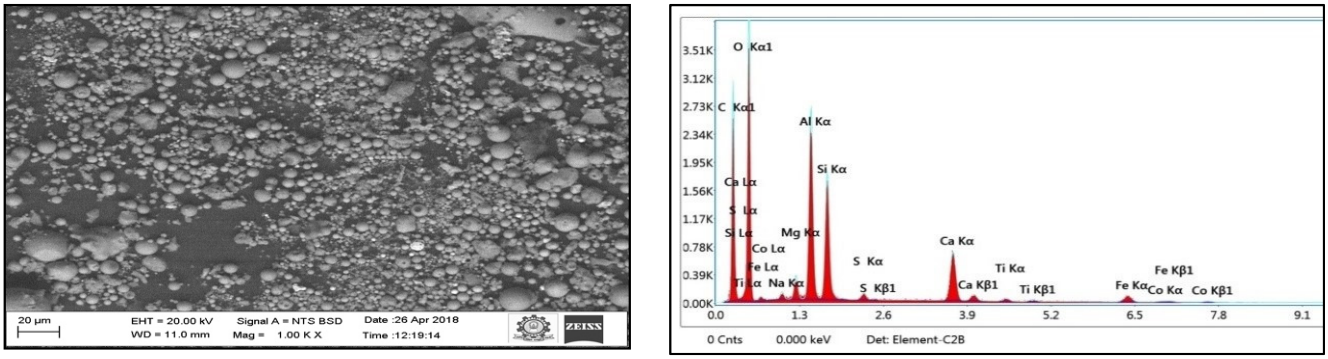

(**a**) (**b**)

Figure 2. (**a**) SEM image of Class C fly ash; (**b**) EDAX image of Class C fly ash.

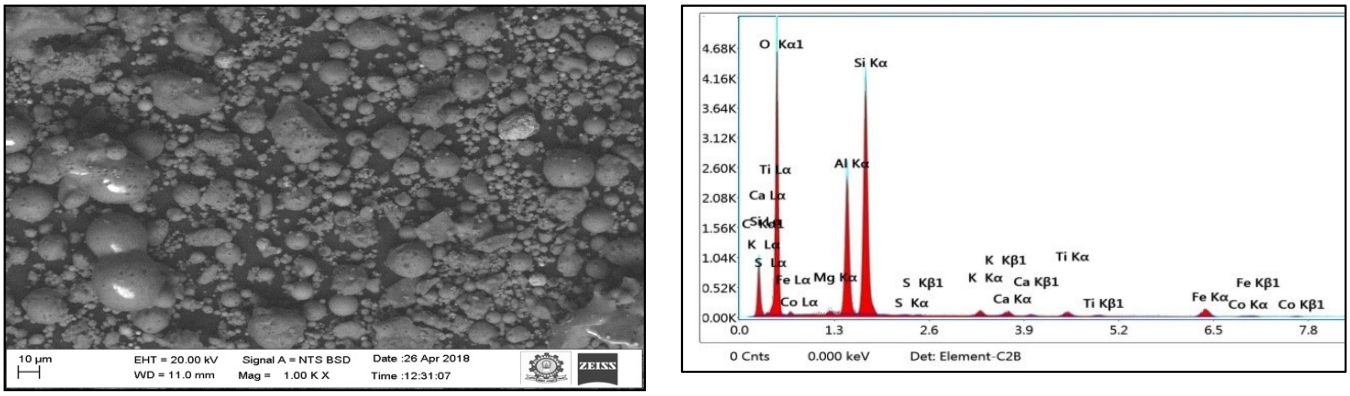

(**a**) (**b**)

Figure 3. (**a**) SEM image of Class F fly ash; (**b**) EDAX image of Class F fly ash.

Table 1. Physical and Chemical compositions of Cement, FA, and GGBS.

Physical Properties					Chemical Compositions				
	Cement	Class C Fly Ash	Class FFly Ash	GGBS	Chemical Component	Cement	Class C Fly Ash	Class FFly Ash	GGBS
Appearance	Grey	Blackish Grey	Grey	White		(Chemical Component, %)			
Specific gravity	3.15	2.6	1.94	2.8	SiO_2	19.15	38.75	59.12	39.17
Bulk density (kg/m^3)	1365	920	996	1200	Fe_2O_3	3.62	12.04	7.14	0.552
Fineness (m^2/kg)	320	421	370	360	Al_2O_3	4.94	13.55	26.2	14.69
-	-	-	-	-	CaO	65.81	16.95	2.74	8.14
-	-	-	-	-	TiO_2	0.78	1.35	1.59	34.15
-	-	-	-	-	SO_3	4.15	13.92	0.314	0.312
-	-	-	-	-	f-CaO	0.60	3.15	0.89	1.21
-	-	-	-	-	P_2O_5	0.03	-	0.03	1.86
-	-	-	-	-	LOI	0.92	0.29	0.87	0.14

Figure 2a,b and Figure 3a,b clearly shows the microscopic structure of the fly ash by scanning electron microscopic analysis (SEM) and chemical components of fly ash were found using (EDAX) images of both Class C & F fly ash utilized in the investigation.

2.3. Lime Powder

Class-C Lime powder confirming to IS: 2541:1991 [51] was used in this study. Generally, lime powder improves the binding properties of aerated concrete. Few researchers reported optimizing lime powder at a range of 5–7% for manufacturing aerated concrete, ex; excessive use of lime powder in concrete leads to drying shrinkage. Therefore 5.5% of lime powder in the entire concrete medium was used in this investigation. Figure 4a,b clearly shows the SEM and EDAX image of lime powder.

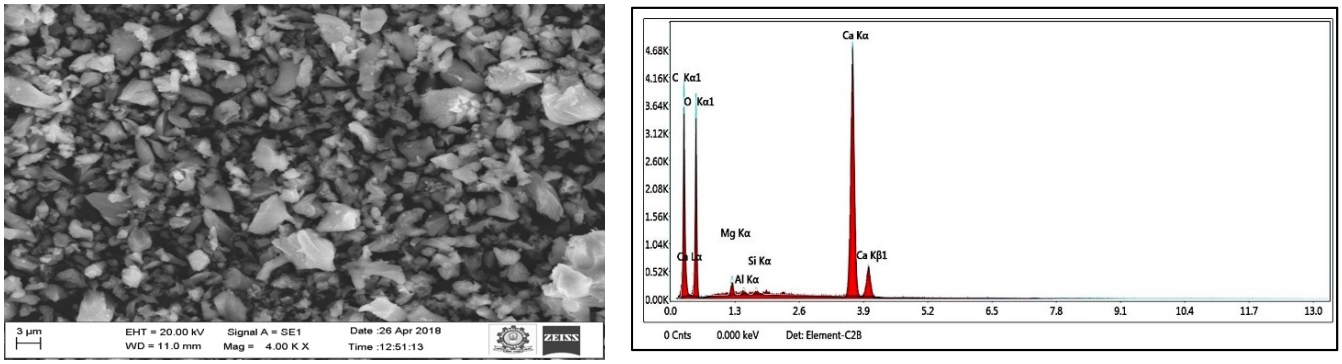

(**a**) (**b**)

Figure 4. (**a**) SEM image of Lime powder; (**b**) EDAX image of Lime powder.

2.4. Gypsum

As per IS: 2542-1978 (Part 1) [52] gypsum plays a major role in controlling the setting time; therefore, 1.5% quantity of gypsum was utilized in the manufacturing process of aerated concrete. Figure 5a,b clearly shows the SEM and EDAX image of gypsum.

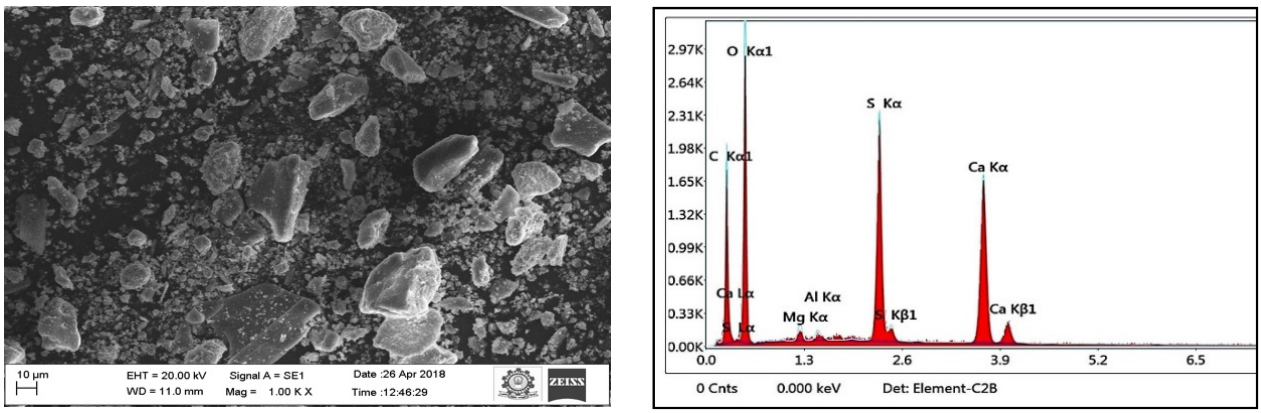

(**a**) (**b**)

Figure 5. (**a**) SEM image of Gypsum; (**b**) EDAX image of Gypsum.

2.5. Aluminum Powder

Aluminum powder is an aerating agent that doubles the volume of the entire concrete matrix; along with soap oil, it plays a major role in aerating wet concrete. The optimum dosage of soap oil is 0.03% and 0.04% aluminum powder were used in this investigation. Excessive usage of aluminum powder leads to strength degradation and pre-specific density in the AAC blocks [53]. Figure 6a,b clearly shows the SEM and EDAX image of Aluminum powder.

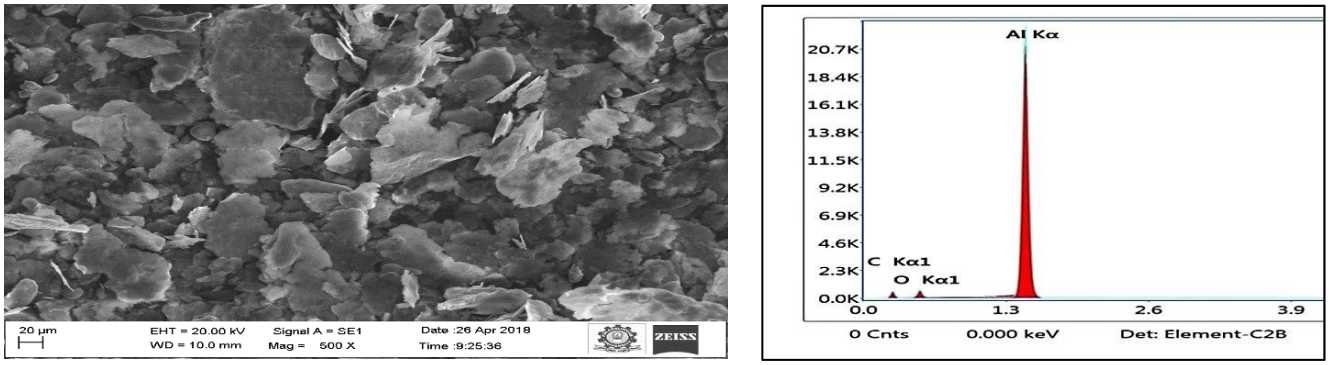

(**a**) (**b**)

Figure 6. (**a**) SEM image of Aluminum Powder; (**b**) EDAX image of Aluminum Powder.

2.6. Ground Granulated Blast Furnace Slag (GGBS)

GGBS is a by-product of blast furnaces that has high cementitious properties. Hence, GGBS was partially replaced for cement in the AAC blocks manufacturing. GGBS has high SiO_2 and CaO, around 70–75%, to enhance the strength of concrete. As confirmed to IS: 12089-1987 [54], the GGBS was used in this investigation. The 0.14% of loss of ignition was observed in the GGBS. Figure 7a,b clearly shows the SEM and EDAX image of GGBS.

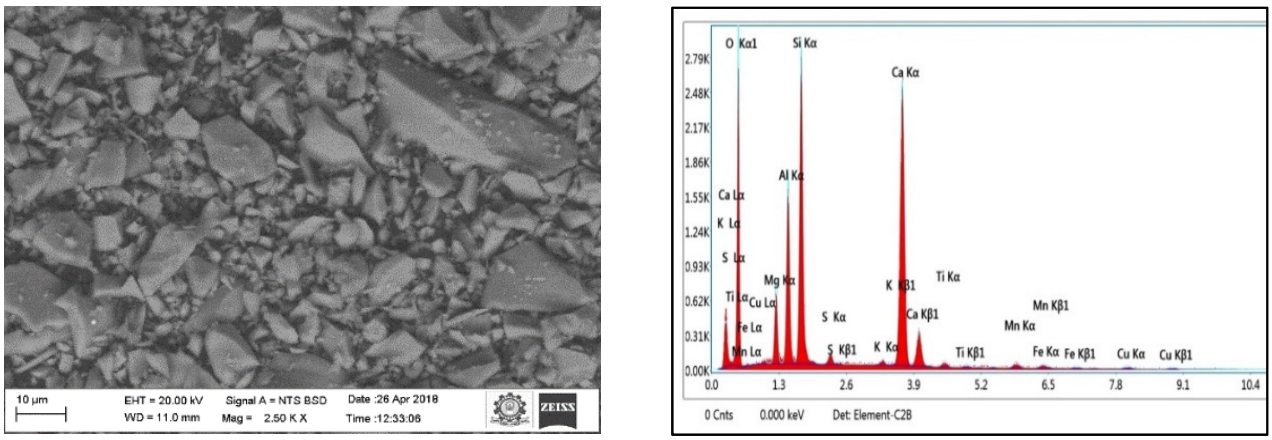

(**a**) (**b**)

Figure 7. (**a**) SEM image of GGBS (**b**) EDAX image of GGBS.

2.7. Water

The amount of water used for the preparation of specimens was determined based on the state of workability of the cementitious paste as per IS: 456-2000 [55]. The amount of water used in this AAC was limited to 26%. When the dosage of water is increased, the reaction between aluminum powder and the wet concrete matrix gets disturbed, and this leads to difficulty in initiating the aeration process in the concrete matrix. Figure 8 shows the raw materials used in AAC.

Figure 8. Raw materials used in AAC.

3. Preparation of Specimens

The AAC Specimen preparation Process is presented in Figure 9. The conventional AAC specimens were prepared with main ingredients like cement, fly ash, lime, gypsum, and soap oil were added together with water, and the slurry was mixed thoroughly by means of a mechanical stirrer. The final aluminum powder was added and the entire matrix was vigorously stirred for about 60 s and the concrete was poured into the casting molds. Figure 10a shows AAC specimens. All the specimens were kept in a pre-curing chamber for about 60 min, as shown in Figure 10b. In the pre-curing chamber, a temperature of about 40–45 °C was maintained. After the pre-curing process, the excess concrete in the specimens was cut down and the molds were removed. The aerated concrete specimens were in a semi-hardened state at that stage. All the specimens were kept in the autoclaving chamber for the final curing process, as shown in Figure 10c. Autoclaving chamber does the steam curing operation in which pressure at a range of 8–12 bars and temperature of the steam up to 180–200 °C is always maintained. The specimens were kept in the autoclaving chamber for about 8–10 h and then taken out for testing [20]. In this study, trial mixes were made to produce conventional AAC having a density in the range of 600 kg/m^3 to 700 kg/m^3 have been prepared. Fly ash conforming to IS: 2542-1978 [56] and IS: 3812-2003 [57] was used. Two different classes of fly ash, namely Class C and Class F fly ash, were used. Class C fly ash incorporated AAC specimens was described as CAAC-C and Class F fly ash incorporated AAC specimens was described as CAAC-F. Both were cast and tested.

A higher volume of SiO_2 makes the concrete mix possess a more cementitious reaction. In this research, the volume of the fly ash used was about 65% to 70% of the entire AAC mix. Fly ash acts as a binder as well as a filler agent for the mass concrete. In sand-based aerated concrete, the cementitious performance is low when compared to that of fly ash-based AAC. In general, fly ash contributes to the secondary hydration process in the concrete.

In this study, GGBS is used as a partial replacement for cement in AAC. The replacement dosage was set from 5% to 20% (5% GGBS + 95% cement, 10% GGBS + 90% cement, 15% GGBS + 85% cement and 20% GGBS + 80% Cement) in this research work.

Table 2 shows the code/description of AAC blocks incorporated using cement were partially replaced using GGBS and fly ash.

Table 2. Designation of specimens.

No	Code/Designation	Description
1	CS	Conventional/Control AAC.
2	5% GGBS + 95% Cement (G5C95)	GGBS incorporated AAC, in which 5% of cement is partially replaced by GGBS.
3	10% GGBS + 90% Cement (G10C90)	GGBS incorporated AAC, in which 10% of cement is partially replaced by GGBS.
4	15% GGBS + 85% Cement (G15C85)	GGBS incorporated AAC, in which 15% of cement is partially replaced by GGBS.
5	20% GGBS + 80% Cement (G20C80)	GGBS incorporated AAC, in which 20% of cement is partially replaced by GGBS.
6	CAAC-C	Class C Fly ash incorporated AAC
7	CAAC-F	Class F Fly ash incorporated AAC

Studies on AAC with fly ash and GGBS include the following mechanical studies such as compressive strength test, modulus of rupture, dry density, and water absorption. In the microstructural studies, investigations were made using SEM, X-ray diffractometer, Energy dispersive X-ray spectrometer, and Fourier-transform infrared spectrophotometer.

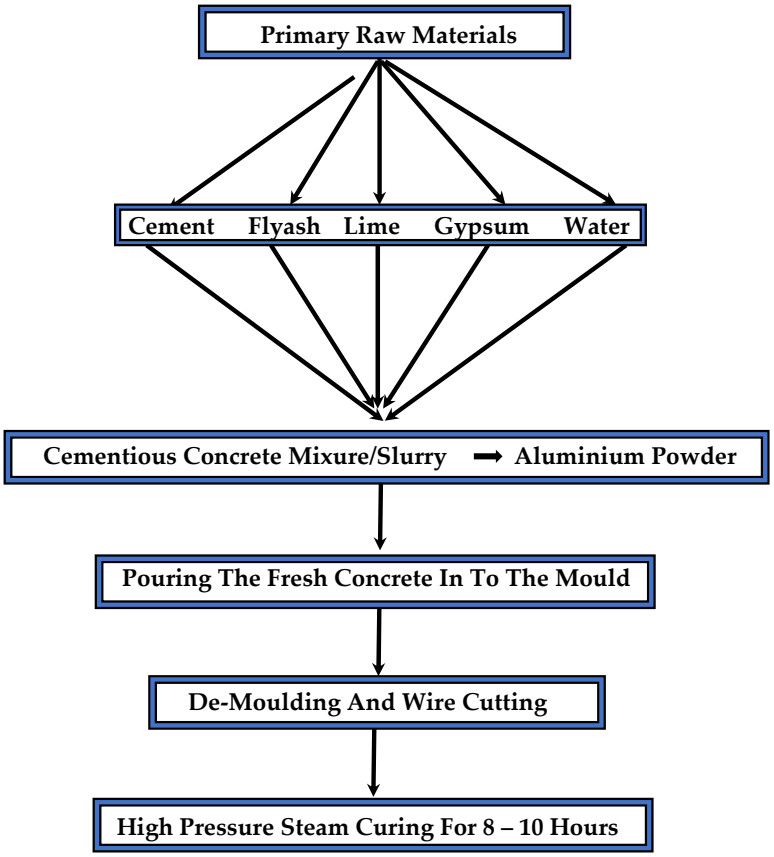

Figure 9. Flow chart of the AAC Specimen Preparation Process.

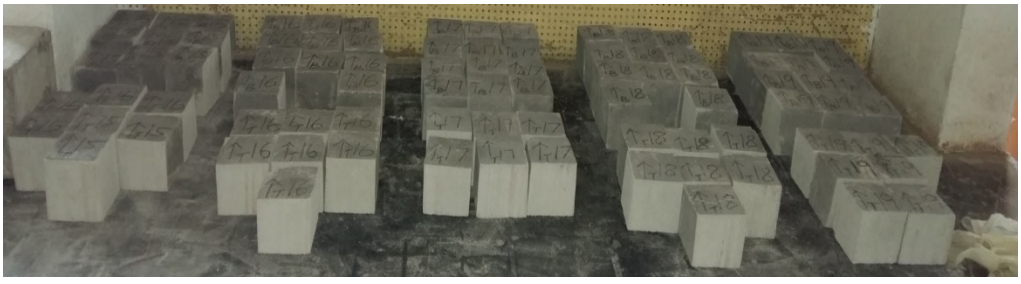

(**a**)

Figure 10. *Cont.*

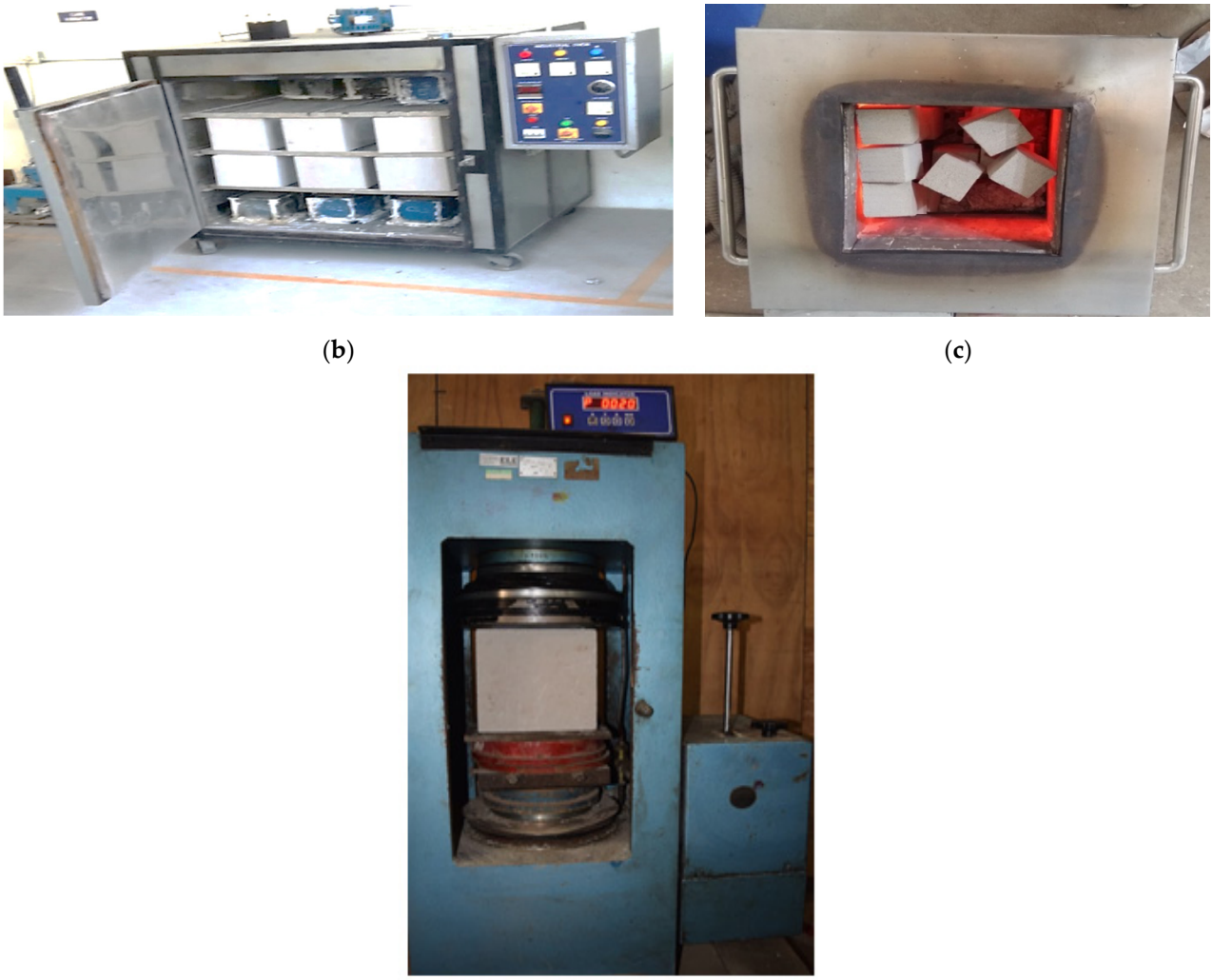

(**b**) (**c**)

(**d**)

Figure 10. (**a**) Specimens used for testing; (**b**) pre-curing of specimens; (**c**) specimens placed in an autoclave; (**d**) compressive strength test.

4. Results and Discussions

The results of experimental studies on the mechanical properties of AAC with fly ash and GGBS are discussed below.

4.1. Compressive Strength

A standard AAC cube size of 150 × 150 × 150 mm was cast and tested according to IS: 2185-1989 [58] to evaluate the cube compressive strength of conventional and GGBS incorporated in concrete with different Class C & F fly ash. The compressive strength test carried out is shown in Figure 10d. Figure 11a clearly shows the compressive strength of conventional AAC and Figure 11b clearly shows the Compressive strength of GGBS incorporated in AAC.

From the test results, we observed Class F fly ash-based AAC compressive strength was around 9% higher than that of Class C fly ash. The presence of a high range of silica in Class F fly ash enhances the compressive strength of conventional aerated concrete when compared to Class C fly ash. For the dosage of GGBS incorporated AAC blocks, the strength increased around 3.6% for G5C95 specimens, 37% strength increased for G10C90 specimens, 68.6% strength increased for G15C85 specimens, and 4% strength decreased for G20C80 specimens.

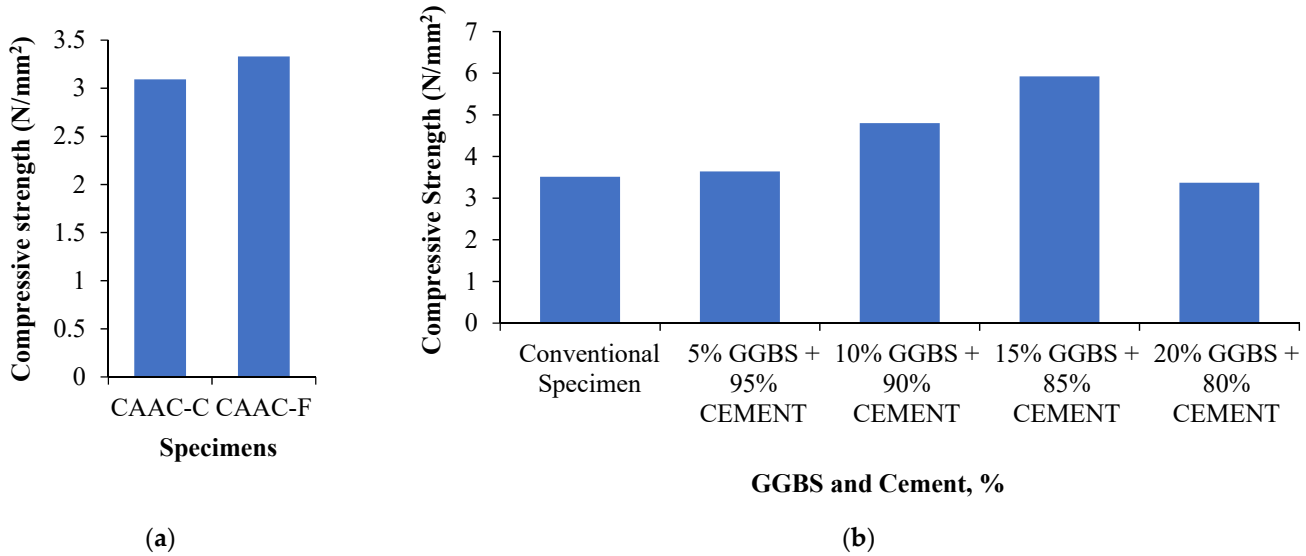

Figure 11. Compressive strength of (**a**) Conventional AAC and (**b**) GGBS incorporated in AAC.

4.2. Modulus of Elasticity

Based on Narayanan and Ramamurthy [53], a modulus of elasticity of AAC have developed to predict.

$$MOE = 1550\ fck^{0.7} \quad (1)$$

Figure 12a clearly shows the modulus of elasticity of conventional AAC and Figure 12b clearly shows the modulus of elasticity of GGBS incorporated in AAC. The performance test was conducted on the AAC to evaluate the elasticity of aerated concrete prepared using Class C &F fly ash. From the test results, Class F fly ash-based AAC has a 5.36% high modulus of elasticity when compared to Class C fly ash incorporated in AAC. For the dosage of GGBS incorporated AAC blocks, the modulus of elasticity increased around 2.56% for G5C95 specimens, 24.5% modulus of elasticity increased for G10C90 specimens, and the highest peak of 44% modulus of elasticity increased for G15C85 specimens, and 3% modulus of elasticity decreased for G20C80 specimens.

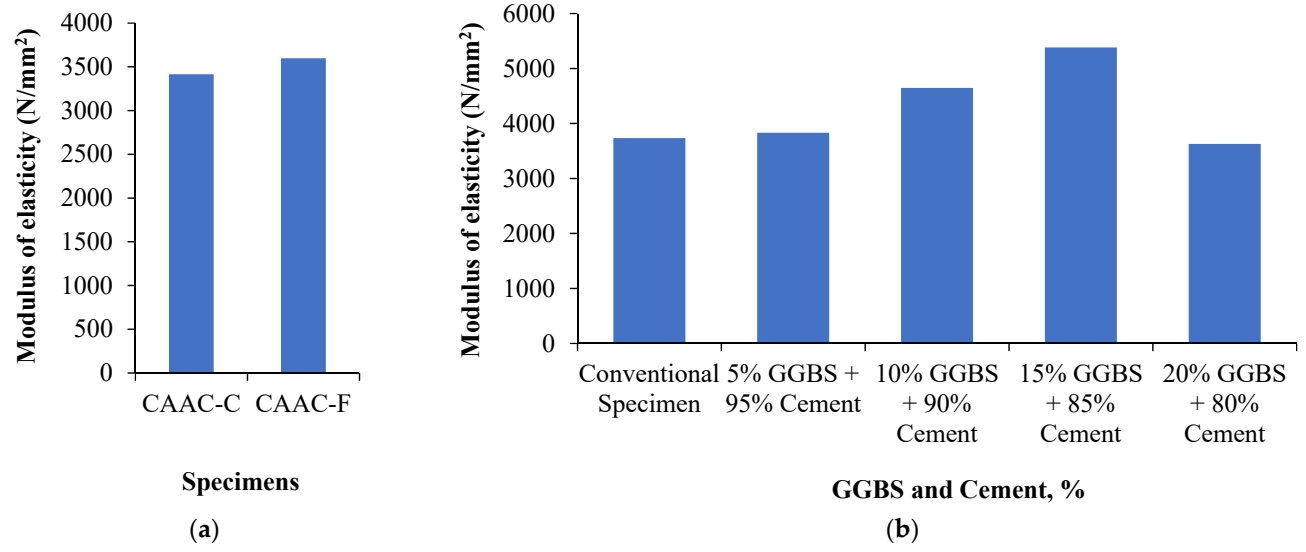

Figure 12. Modulus of Elasticity of (**a**) Conventional AAC and (**b**) GGBS incorporated in AAC.

4.3. Modulus of Rupture

Modulus of rupture is one of the important parameters in the AAC prism. Now a day's large size prism is tested to understand the behavior in AAC prism using different fly ash content [59,60]. In this investigation, Class F & C fly ash was tested with single point load to understand the failure mechanism of AAC prism. The flexure test was performed to understand the behavior of the AAC prism. It was found the specimens failed due to brittle. Figure 13 clearly shows the modulus of rupture experimental setup and schematic view. Figure 14a clearly shows the modulus of rupture of conventional AAC and Figure 14b clearly shows the modulus of rupture of GGBS incorporated in AAC.

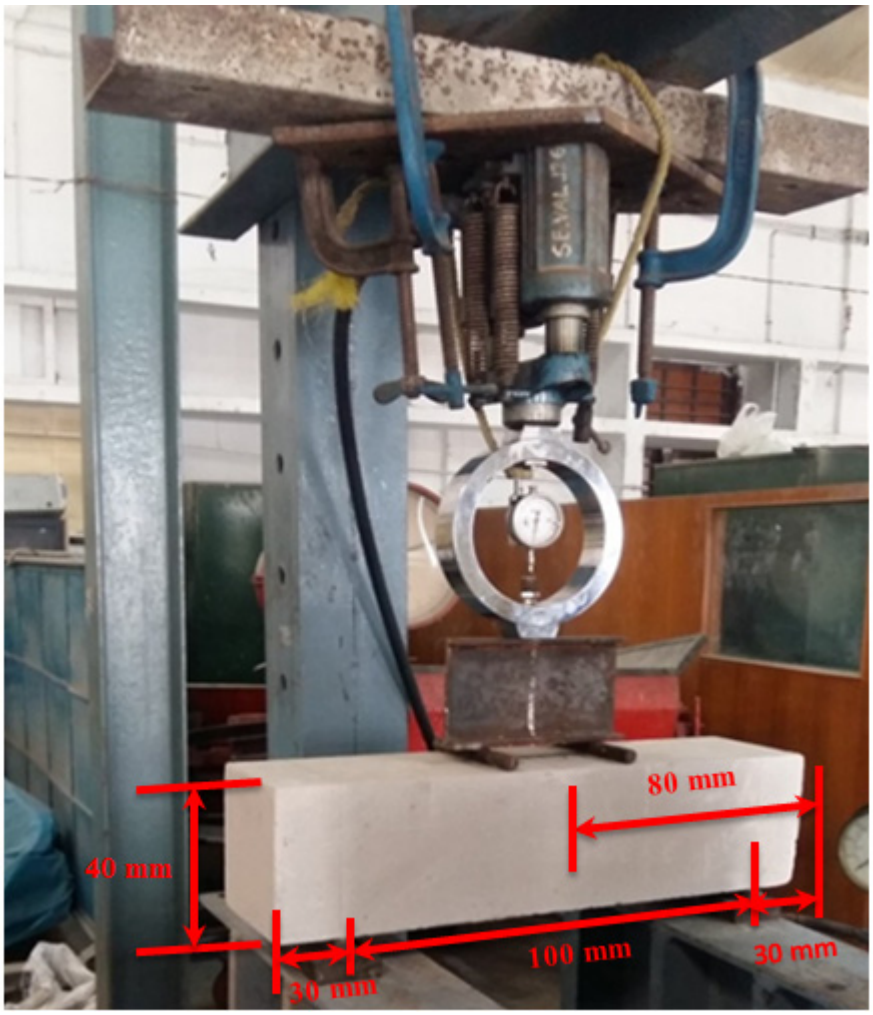

Figure 13. Depiction view of the modulus of rupture experimental test setup.

From the test results, it was observed that Class F fly ash has a 5.44% higher modulus of rupture capacity than that of Class C fly ash-based AAC. The modulus of rupture value was found to be very low when compared to conventional concrete because of its low strength and low density of the materials used to manufacture the aerated concrete specimen. For the dosage of GGBS incorporated AAC blocks, the modulus of rupture increased by around 2.66% for G5C95 specimens, 26.85% modulus of rupture increased for G10C90 specimens, the highest peak 50.23% modulus of rupture increased for G15C85 specimens, and 3% modulus of rupture decreased for G20C80 specimens. From the results of compressive strength, modulus of Elasticity, and modulus of Rupture, it is concluded that when GGBS increases, the ratio of GGBS to cement will also increase, and the calcium hydroxide from cement hydration is utilized completely, resulting in excess GGBS that behaves as an inert filler and reduces the compressive strength and elasticity of the concrete.

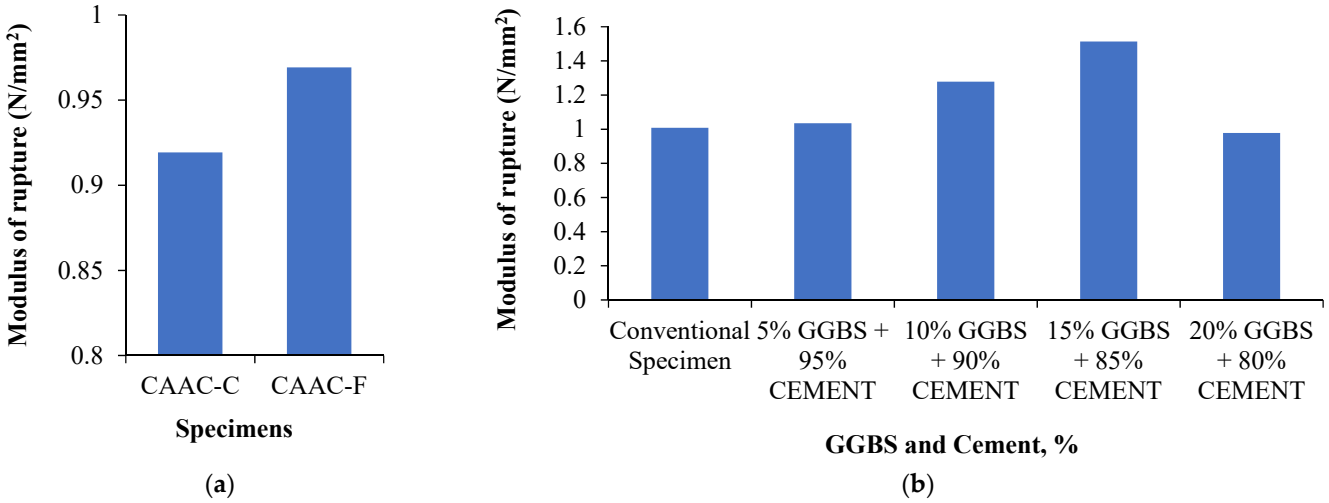

Figure 14. Modulus of rupture of (**a**) Conventional AAC and (**b**) GGBS incorporated in AAC.

4.4. Dry Density

To find out the dry density of the AAC, the specimens are kept at 500 °C for 30 min in the hot air oven. The excess moisture content in the voids of AAC is removed by providing temperature. After treating the AAC specimens in the hot air oven for 30 min at 500 °C, the dry density ranges for conventional AAC was around 665 kg/m^3 to 670 kg/m^3 and the dry density for GGBS was incorporated AAC was around 635 to 655 kg/m^3. Figure 15a clearly shows the dry density of conventional AAC and Figure 15b clearly shows the dry density of GGBS incorporated in AAC.

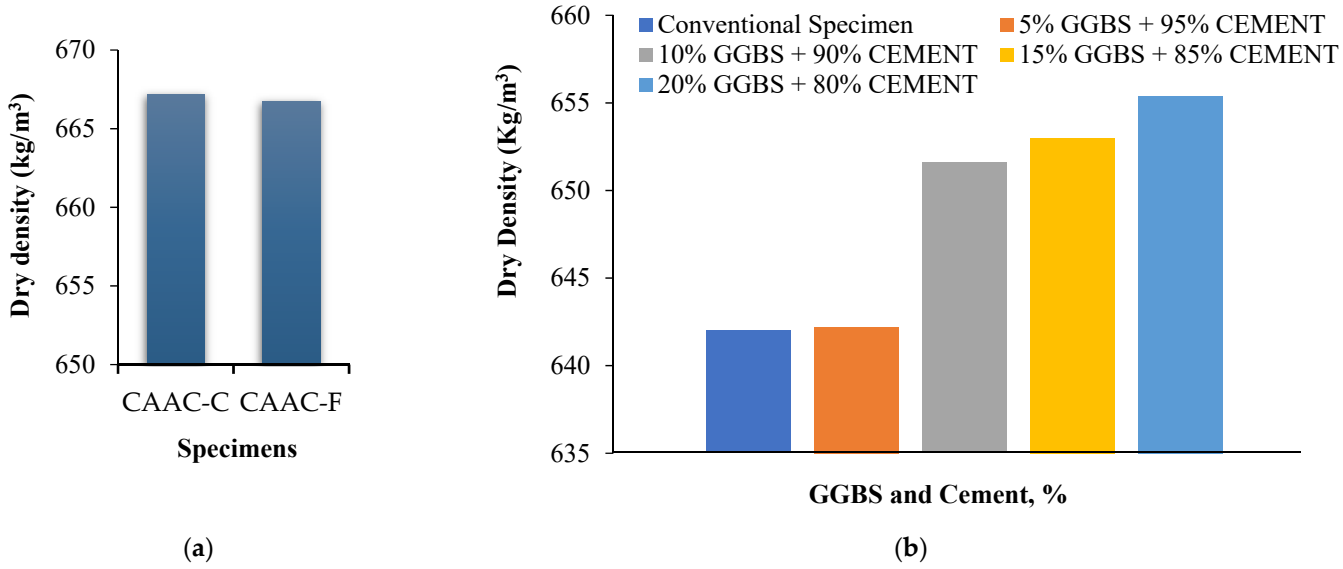

Figure 15. Dry density of (**a**) Conventional AAC and (**b**) GGBS incorporated in AAC.

4.5. Water Absorption

The percentage of water absorption in AAC is very high when compared to conventional concrete blocks. In general, Class C & F fly ash AAC blocks water absorption for conventional AAC was in the range of 18 to 20% and water absorption for GGBS incorporated AAC was in the range of 19% for all the dosages. Figure 16 clearly shows the water absorption of conventional AAC and Figure 17 clearly shows the water absorption of GGBS incorporated in AAC. The AAC specimen is generally less dense so that it floats in the water, but it observes more water when compared to conventional concrete blocks. To determine the water absorption capacity of the AAC blocks, they have to be immersed

fully in the water; hence, the AAC blocks are pressurized into the container with water. Comparing the dry density and water absorption of the specimens, there is no correlation between the dry density and water absorption. As the water absorption remains to be the same for all percentage replacements of GGBS, whereas dry density varies with respect to replacements percentages of GGBS.

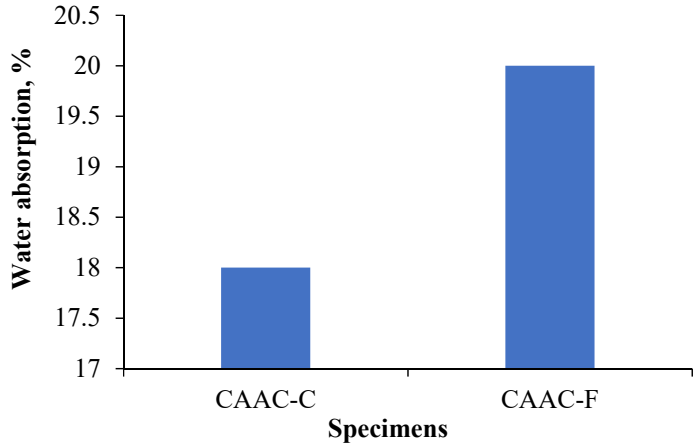

Figure 16. Water absorption of conventional AAC.

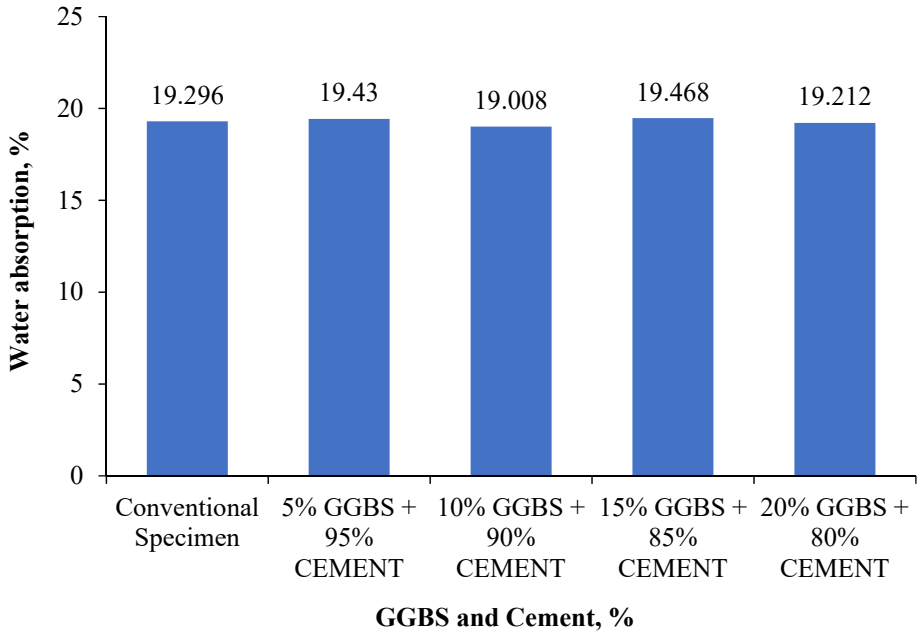

Figure 17. Water absorption of GGBS incorporated in AAC.

4.6. Scanning Electron Microscope (SEM)

In this investigation, SEM analysis was performed on conventional AAC blocks and incorporated with GGBS was partially replaced for the cement. There are no significant changes observed in the structural morphology using SEM analysis on the Class C & F-based AAC blocks comprised of 15% GGBS and 85% cement. The formation of tobermorite is high in GGBS incorporated AAC block when compared to conventional AAC block because of the high concentration of silicon dioxide (SiO_2) and calcium oxide (CaO) present in the GGBS. Figure 18 clearly shows the SEM image of AAC specimens when using a conventional AAC of Class C fly ash, conventional AAC of Class F fly ash (CAAC-F), and GGBS with 85% cement in AAC block using 15% fly ash.

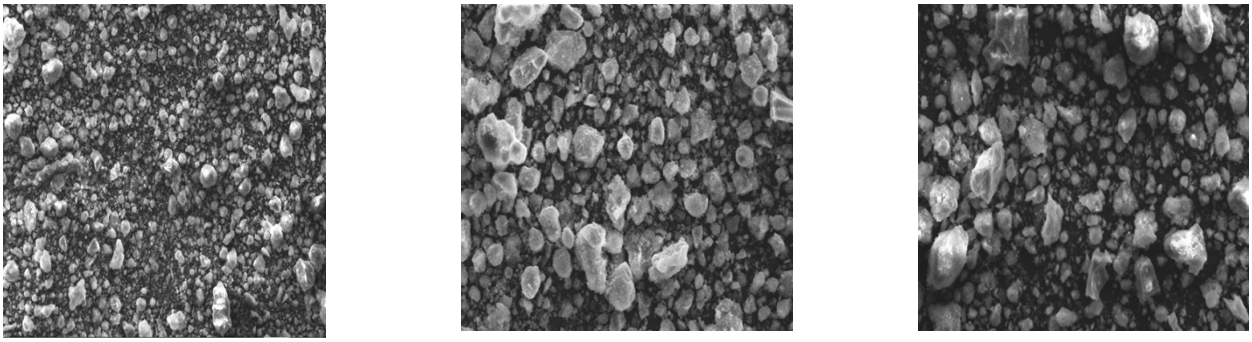

(**a**) (**b**) (**c**)

Figure 18. SEM images of AAC specimens: (**a**) CAAC-C, (**b**) CAAC-F, (**c**) GGBS-CE-AAC-F.

4.7. X-ray Diffractometer

In this investigation, an XRD test was conducted on AAC conventional and AAC incorporated with GGBS as a partial replacement of cement. The optimized mix incorporated GGBS aerated concrete was 15% of GGBS + 85% Cement. This is an XRD analysis of optimized mix AAC of different specimens such as CAAC-C, CAAC-F, and GGBS-CE-AAC-F. The XRD results clearly show both the conventional and GGBS incorporated AAC possess similar diffracted images. Figure 19 clearly shows the XRD image of AAC specimens.

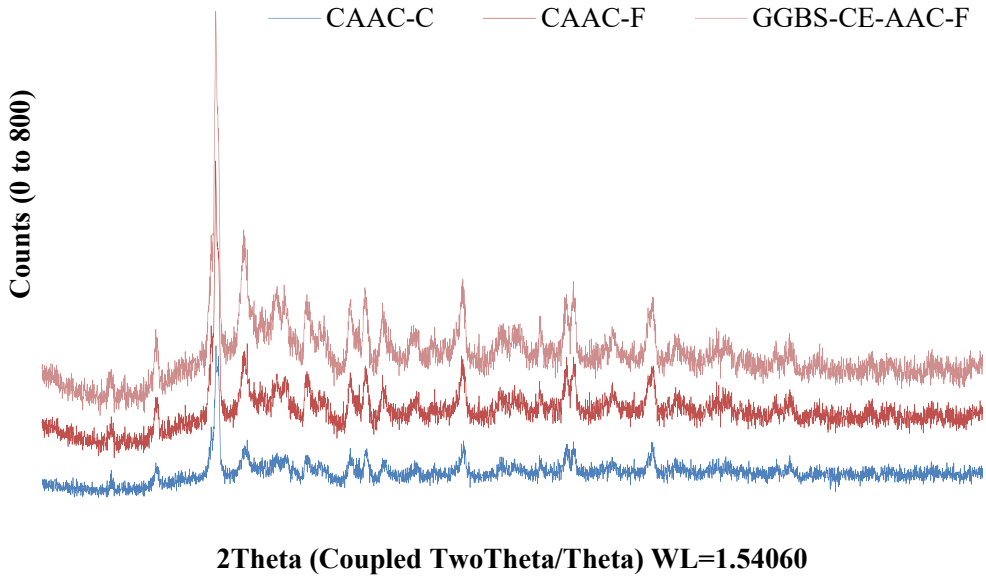

Figure 19. XRD image of AAC specimens.

The results obtained from XRD clearly show that conventional AAC and GGBS incorporated AAC possess a similar pattern. However, the formation of tobermorite, quartz, and anhydrites were found to be higher in GGBS incorporated AAC when compared to conventional AAC blocks. Due to the presence of SiO_2 and CaO in GGBS incorporated AAC, it shows a higher strength capacity.

4.8. Energy Dispersive X-ray Spectrometer (EDAX)

To identify the chemical composition of AAC with different combinations, an EDAX analysis was performed. The presence of silicon and calcium tends to have high strength when compared to conventional AAC blocks. Figure 20 clearly shows the EDAX image of AAC specimens.

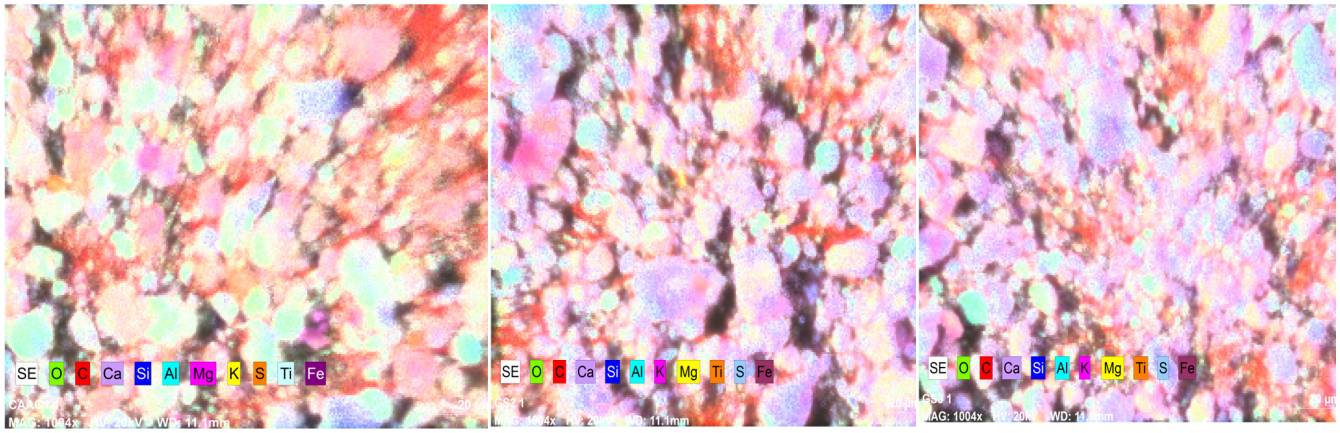

(**a**) (**b**) (**c**)

Figure 20. EDAX images of AAC specimens: (**a**) CAAC-C, (**b**) CAAC-F, (**c**) GGBS-CE-AAC-F.

The distribution of chemicals in AAC conventional and incorporated GGBS was found to be similar but the strength of GGBS incorporated was higher than in conventional AAC. The main reason behind the increase in strength is due to the presence of Silicon dioxide (SiO_2) and Calcium oxide (CaO) in GGBS.

4.9. Fourier Transform Infra-Red Spectrophotometer (FTIR)

FTIR spectroscopy is mainly used in this investigation to identify compounds in the concrete. To determine the functional group on AAC specimens, FTIR analysis was performed. The FTIR results were obtained for AAC incorporated with different materials and are plotted in Figure 21.

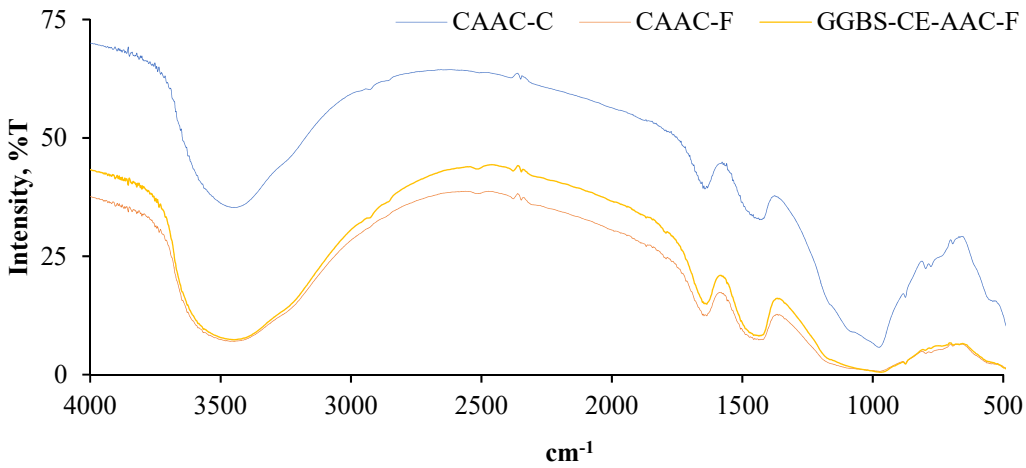

Figure 21. FTIR results of AAC specimens.

The change in the functional group was observed when an external raw material was incorporated into the concrete. The optimized dosage of 15% GGBS + 85% Cement was utilized for the FTIR analysis. As GGBS contains cementitious property, although there are no huge changes in the FTIR results. Hence, the 15% GGBS replacement of cement can be considered to improve the strength and durability properties of AAC blocks.

5. Conclusions

Autoclaved Aerated Concrete (AAC) is a lightweight cellular concrete, which includes sand-based AAC and fly ash-based AAC. In this research, studies on fly ash-based AAC have been carried out. The primary objective of this research was to investigate the performance of AAC using industrial wastes (e.g., GGBD and fly ash). At first, the raw

materials were collected and their physical and chemical properties were tested. Then, AAC specimens of each containing Class-C fly ash, Class-F fly ash, and GGBS with the replacement dosages from 5% to 20% (5% GGBS + 95% Cement, 10% GGBS + 90% Cement, 15% GGBS + 85% cement, and 20% GGBS + 80% Cement) were prepared and its mechanical and thermal properties were studied along with microstructural investigation using SEM, XRD, EDAX, and FTIR for all of the varied dosages. The following conclusions were drawn from the experimental investigations, which focused on the mechanical properties of AAC conventional and the incorporation of GGBS.

- The average dry density of Class C and F fly ash was found to be similar in behavior but slightly different in the values of 665 kg/m^3 to 675 kg/m^3. The reduction around 635 kg/m^3 to 655 kg/m^3 was found when the incorporation of 15% GGBS + 85%.
- The compressive strength of Class F fly ash-based AAC conventional possesses 7 to 9% higher strength when compared to Class C fly ash. The higher strength was obtained for Class F fly ash AAC due to the presence of 59% of SiO_2. Furthermore, incorporation of 15% GGBS + 85% Cement increases the compressive strength up to 68.6%.
- The modulus of elasticity and modulus of rupture of Class F fly ash-based AAC was 5.36% and 5.44% higher when compared to Class C fly ash.
- The water absorption of Class C and F fly ash-based AAC was in the range of 18% to 20%.
- The overall performance of Class F fly ash AAC tends to be significant in all the performed tests and hence it is recommended to use Class F fly ash in the manufacturing of AAC blocks.
- The incorporation of GGBS in the manufacturing process would increase the compressive strength of concrete. Hence it is recommended to use 15% GGBS + 85% cement as a potential rate of replacement to improve the mechanical properties of AAC blocks significantly.

Author Contributions: Conceptualization, V.A.R.B., S.M.R. and C.U.; data curation, V.A.R.B., S.M.R., S.A., C.U., M.A., P.G., R.F. and N.I.V.; formal analysis, V.A.R.B., S.M.R., S.A., C.U., M.A., P.G., R.F. and N.I.V.; funding acquisition, M.A., R.F. and N.I.V.; investigation, V.A.R.B. and S.M.R.; methodology, V.A.R.B., S.M.R. and C.U.; project administration, N.I.V.; resources, S.A., C.U., M.A., P.G., R.F. and N.I.V.; software, V.A.R.B., S.A. and C.U.; Supervision, S.M.R., S.A. and C.U.; validation, S.M.R., S.A., C.U., M.A., P.G., R.F. and N.I.V.; visualization, M.A., R.F. and N.I.V.; writing—original draft, V.A.R.B.; writing—review & editing, S.M.R., S.A., C.U., M.A., P.G., R.F. and N.I.V. All authors have read and agreed to the published version of the manuscript.

Funding: The research is partially funded by the Ministry of Science and Higher Education of the Russian Federation under the strategic academic leadership program 'Priority 2030' (Agreement 075-15-2021-1333 dated 30 September 2021).

Institutional Review Board Statement: Not applicable.

Informed Consent Statement: Not applicable.

Data Availability Statement: Not applicable.

Acknowledgments: The authors acknowledge the Department of Civil Engineering, College of Engineering Guindy, Anna University Chennai, for their financial support for the experimental works. Centro Nacional de Excelencia para la Industria de la Madera (ANID BASAL FB210015 CENAMAD), Pontificia Universidad Católica de Chile, Vicuña Mackenna 7860, Santiago, Chile. The authors also gratefully acknowledge the financial support given by the Deanship of Scientific Research at Prince Sattam bin Abdulaziz University, Alkharj, Saudi Arabia, for this research.

Conflicts of Interest: The authors declare no conflict of interest.

References

1. Saiyed, F.M.; Makwana, A.H.; Pitroda, J.; Vyas, C.M. Aerated Autoclaved Concrete (AAC) Blocks : Novel Material for Construction Industry. *Int. J. Adv. Res. Eng. Sci. Manag.* **2014**, *I*, 21–32.
2. Aylsworth, J.W.; Dyer, F.L. Porous artificial stone and its production. *USA Pat. Off.* **1994**, *28*, 131–134. [CrossRef]
3. Rahman, R.A.; Fazlizan, A.; Asim, N.; Thongtha, A. A review on the utilization of waste material for autoclaved aerated concrete production. *J. Renew. Mater.* **2021**, *9*, 61–72. [CrossRef]
4. Amran, Y.H.M.; Farzadnia, N.; Ali, A.A.A. Properties and applications of foamed concrete; A review. *Constr. Build. Mater.* **2015**, *101*, 990–1005. [CrossRef]
5. Amran, M.; Onaizi, A.M.; Fediuk, R.; Danish, A.; Vatin, N.I.; Murali, G.; Azevedo, A. An ultra-lightweight cellular concrete for geotechnical applications–A review. *Case Stud. Constr. Mater.* **2022**, *16*, e01096. [CrossRef]
6. Fedyuk, R.S.; Baranov, A.; Mugahed Amran, Y.H. Effect of Porous Structure on Sound Absorption of Cellular Concrete. *Constr. Mater. Prod.* **2020**, *3*, 5–18. [CrossRef]
7. Qu, X.; Zhao, X. Previous and present investigations on the components, microstructure and main properties of autoclaved aerated concrete–A review. *Constr. Build. Mater.* **2017**, *135*, 505–516. [CrossRef]
8. Cai, L.; Ma, B.; Li, X.; Lv, Y.; Liu, Z.; Jian, S. Mechanical and hydration characteristics of autoclaved aerated concrete (AAC) containing iron-tailings: Effect of content and fineness. *Constr. Build. Mater.* **2016**, *128*, 361–372. [CrossRef]
9. Aroni, S.; RILEM Technical Committee 78-MCA; RILEM Technical Committee 51-ALC. *Autoclaved Aerated Concrete: Properties, Testing, and Design: RILEM Recommended Practice*; E & FN Spon: London, UK; New York, NY, USA, 1993; ISBN 9780203626689.
10. Chaipanich, A.; Chindaprasirt, P. The properties and durability of autoclaved aerated concrete masonry blocks. In *Eco-Efficient Masonry Bricks and Blocks: Design, Properties and Durability*; Woodhead Publishing: Sawston, UK, 2015; pp. 215–230. ISBN 9781782423188.
11. Susan Raj, I.; Darsh, M.S.J.; John, E. Review on properties of GGBFS and fly ash incorporated aerated concrete with filler materials. *Sustain. Agric. Food Environ. Res.* **2021**, *10*. [CrossRef]
12. Amran, M.; Fediuk, R.; Vatin, N.; Lee, Y.H.; Murali, G.; Ozbakkaloglu, T.; Klyuev, S.; Alabduljabber, H. Fibre-reinforced foamed concretes: A review. *Materials* **2020**, *13*, 4323. [CrossRef]
13. Song, Y.; Li, B.; Yang, E.H.; Liu, Y.; Ding, T. Feasibility study on utilization of municipal solid waste incineration bottom ash as aerating agent for the production of autoclaved aerated concrete. *Cem. Concr. Compos.* **2015**, *56*, 51–58. [CrossRef]
14. Matsui, K.; Kikuma, J.; Tsunashima, M.; Ishikawa, T.; Matsuno, S.Y.; Ogawa, A.; Sato, M. In situ time-resolved X-ray diffraction of tobermorite formation in autoclaved aerated concrete: Influence of silica source reactivity and Al addition. *Cem. Concr. Res.* **2011**, *41*, 510–519. [CrossRef]
15. Loganina, V.; Davydova, O.; Fediuk, R.; Amran, M.; Klyuev, S.; Klyuev, A.; Sabitov, L.; Nabiullina, K. Improving the Durability of Lime Finishing Mortars by Modifying Them with Silicic Acid Sol. *Materials* **2022**, *15*, 2360. [CrossRef] [PubMed]
16. Subash, N.; Avudaiappan, S.; Adish Kumar, S.; Amran, M.; Vatin, N.; Fediuk, R.; Aepuru, R. Experimental Investigation on Geopolymer Concrete with Various Sustainable Mineral Ashes. *Materials* **2021**, *14*, 7596. [CrossRef]
17. Amran, M.; Huang, S.S.; Debbarma, S.; Rashid, R.S.M. Fire resistance of geopolymer concrete: A critical review. *Constr. Build. Mater.* **2022**, *324*, 126722. [CrossRef]
18. Narayanan, N.; Ramamurthy, K. Microstructural investigations on aerated concrete. *Cem. Concr. Res.* **2000**, *30*, 457–464. [CrossRef]
19. Hartmann, A.; Schulenberg, D.; Buhl, J.-C. Investigation of the Transition Reaction of Tobermorite to Xonotlite under Influence of Additives. *Adv. Chem. Eng. Sci.* **2015**, *5*, 197–214. [CrossRef]
20. Vijay Antony Raj, B.; Gunasekaran, U.; Ambily, P.S. Experimental investigation on high volume fly ash based autoclaved aerated concrete reinforced with synthetic fibers. *J. Struct. Eng.* **2017**, *44*, 158–169.
21. Muthu Kumar, E.; Ramamurthy, K. Effect of fineness and dosage of aluminium powder on the properties of moist-cured aerated concrete. *Constr. Build. Mater.* **2015**, *95*, 486–496. [CrossRef]
22. Onur Pehlivanlı, Z.; Uzun, İ. Effect of polypropylene fiber length on mechanical and thermal properties of autoclaved aerated concrete. *Constr. Build. Mater.* **2022**, *322*, 126506. [CrossRef]
23. Rafiza, A.R.; Fazlizan, A.; Thongtha, A.; Asim, N.; Noorashikin, M.S. The Physical and Mechanical Properties of Autoclaved Aerated Concrete (AAC) with Recycled AAC as a Partial Replacement for Sand. *Buildings* **2022**, *12*, 60. [CrossRef]
24. Walczak, P.; Szymański, P.; Rózycka, A. Autoclaved Aerated Concrete based on Fly Ash in Density 350kg/m3 as an Environmentally Friendly Material for Energy-Efficient Constructions. *Procedia Eng.* **2015**, *122*, 39–46. [CrossRef]
25. Kunchariyakun, K.; Asavapisit, S.; Sinyoung, S. Influence of partial sand replacement by black rice husk ash and bagasse ash on properties of autoclaved aerated concrete under different temperatures and times. *Constr. Build. Mater.* **2018**, *173*, 220–227. [CrossRef]
26. Yang, J.; Wang, F.; He, X.; Su, Y.; Wang, T.; Ma, M. Potential usage of porous autoclaved aerated concrete waste as eco-friendly internal curing agent for shrinkage compensation. *J. Clean. Prod.* **2021**, *320*, 128894. [CrossRef]
27. Peng, Y.; Liu, Y.; Zhan, B.; Xu, G. Preparation of autoclaved aerated concrete by using graphite tailings as an alternative silica source. *Constr. Build. Mater.* **2021**, *267*, 121792. [CrossRef]
28. Lesovika, V.S.; Ahmed, A.A.; Fediuk, R.S.; Kozlenko, B.; Amran, Y.H.M.; Alaskhanov, A.K.; Asaad, M.A.; Murali, G.; Uvarov, V.A. Performance investigation of demolition wastes-based concrete composites. *Mag. Civ. Eng.* **2021**, *106*, 74–83. [CrossRef]

29. Afiq, M.; Abdullah, H.; Saifulnaz, R.; Rashid, M.; Amran, M.; Hejazii, F.; Azreen, N.; Masenwat, B.; Fediuk, R.; Voo, Y.L.; et al. Recent Trends in Advanced Radiation Shielding Concrete for Construction of Facilities : Materials and Properties. *Polymers* **2022**, *14*, 2830.
30. Arularasi, V.; Pachiappan, T.; Avudaiappan, S.; Raman, S.N.; Guindos, P.; Amran, M.; Fediuk, R.; Vatin, N.I. Effects of Admixtures on Energy Consumption in the Process of Ready-Mixed Concrete Mixing. *Materials* **2022**, *15*, 4143. [CrossRef]
31. Chakrawarthi, V.; Dharmar, B.; Avudaiappan, S.; Amran, M.; Flores, E.S.; Alam, M.A.; Fediuk, R.; Vatin, N.I.; Rashid, R.S.M. Destructive and Non-Destructive Testing of the Performance of Copper Slag Fiber-Reinforced Concrete. *Materials* **2022**, *15*, 4536. [CrossRef]
32. Karmegam, A.; Avudaiappan, S.; Amran, M.; Guindos, P.; Vatin, N.I.; Fediuk, R. Retrofitting RC beams using high-early strength alkali-activated concrete. *Case Stud. Constr. Mater.* **2022**, *17*, e01194. [CrossRef]
33. Arularasi, V.; Thamilselvi, P.; Avudaiappan, S.; Flores, E.I.S.; Amran, M.; Fediuk, R.; Vatin, N.; Karelina, M. Rheological behavior and strength characteristics of cement paste and mortar with fly ash and GGBS admixtures. *Sustainability* **2021**, *13*, 9600. [CrossRef]
34. Abdelgader, H.S.; Kurpińska, M.; Amran, M. Effect of slag coal ash and foamed glass on the mechanical properties of two-stage concrete. *Mater. Today Proc.* **2022**, *58*, 1091–1097. [CrossRef]
35. Raju, S.; Rathinam, J.; Dharmar, B.; Rekha, S.; Avudaiappan, S.; Amran, M.; Ramamoorthy, V.R. Cyclically Loaded Copper Slag Admixed Reinforced Concrete Beams with Cement Partially Replaced with Fly Ash. *Materials* **2022**, *15*, 3101. [CrossRef]
36. Tang, Y.X.; Lee, Y.H.; Amran, M.; Fediuk, R.; Vatin, N.; Kueh, A.B.H.; Lee, Y.Y. Artificial Neural Network-Forecasted Compression Strength of Alkaline-Activated Slag Concretes. *Sustainability* **2022**, *14*, 5214. [CrossRef]
37. Amran, M.; Murali, G.; Khalid, N.H.A.; Fediuk, R.; Ozbakkaloglu, T.; Lee, Y.H.; Haruna, S.; Lee, Y.Y. Slag uses in making an ecofriendly and sustainable concrete: A review. *Constr. Build. Mater.* **2021**, *272*, 121942. [CrossRef]
38. Chakrawarthi, V.; Avudaiappan, S.; Amran, M.; Dharmar, B.; Raj Jesuarulraj, L.; Fediuk, R.; Aepuru, R.; Vatin, N.; Saavedra Flores, E. Impact Resistance of Polypropylene Fibre-Reinforced Alkali–Activated Copper Slag Concrete. *Materials* **2021**, *14*, 7735. [CrossRef] [PubMed]
39. Pachideh, G.; Gholhaki, M. Effect of pozzolanic materials on mechanical properties and water absorption of autoclaved aerated concrete. *J. Build. Eng.* **2019**, *26*, 100856. [CrossRef]
40. Amran, M.; Murali, G.; Fediuk, R.; Vatin, N.; Vasilev, Y.; Abdelgader, H. Palm oil fuel ash-based eco-efficient concrete: A critical review of the short-term properties. *Materials* **2021**, *14*, 332. [CrossRef]
41. Amran, M.; Al-Fakih, A.; Chu, S.H.; Fediuk, R.; Haruna, S.; Azevedo, A.; Vatin, N. Long-term durability properties of geopolymer concrete: An in-depth review. *Case Stud. Constr. Mater.* **2021**, *15*, e00661. [CrossRef]
42. Amran, M.; Fediuk, R.; Abdelgader, H.S.; Murali, G.; Ozbakkaloglu, T.; Lee, Y.H.; Lee, Y.Y. Fiber-reinforced alkali-activated concrete: A review. *J. Build. Eng.* **2022**, *45*, 103638. [CrossRef]
43. Lesovik, V.; Volodchenko, A.; Fediuk, R.; Mugahed Amran, Y.H. Improving the Hardened Properties of Nonautoclaved Silicate Materials Using Nanodispersed Mine Waste. *J. Mater. Civ. Eng.* **2021**, *33*, 04021214. [CrossRef]
44. Avudaiappan, S.; Prakatanoju, S.; Amran, M.; Aepuru, R. Experimental Investigation and Image Processing to Predict the Properties of Concrete with the Addition of Nano Silica and Rice Husk Ash. *Crystals* **2021**, *11*, 1230. [CrossRef]
45. Muthalvan, R.S.; Ravikumar, S.; Avudaiappan, S.; Amran, M.; Aepuru, R.; Vatin, N.; Fediuk, R. The Effect of Superabsorbent Polymer and Nano-Silica on the Properties of Blended Cement. *Crystals* **2021**, *11*, 1394. [CrossRef]
46. Nelubova, V.; Strokova, V.; Fediuk, R.; Amran, M.; Vatin, N.; Vasilev, Y. Effect of an aluminosilicate disperse additive on behaviors of autoclave silicate materials. *Buildings* **2021**, *11*, 239. [CrossRef]
47. Amran, M.; Huang, S.-S.; Onaizi, A.M.; Murali, G.; Abdelgader, H.S. Fire spalling behavior of high-strength concrete: A critical review. *Constr. Build. Mater.* **2022**, *341*, 127902. [CrossRef]
48. *IS 12269*; 2013 Ordinary Portland Cement, 53 Grade Specification. Bureau of Indian Standards: Delhi, India, 2013; pp. 1–14.
49. *IS: 4031*; (Part 6) Methods Of Physical Tests for Hydraulic Cement Part 6 Determination of Compressive Strength of Hydraulic Cement Other Than Masonry Cement (First Revision). Bureau of Indian Standards: Delhi, India, 2005; pp. 1–3.
50. Grutzeck, M.W.; Kwan, S.; Dicola, M. Alkali Activated Autoclaved Aerated Concrete Made with Fly Ash Derived Cenospheres : Effect of Fly Ash and Precuring Temperature. In Proceedings of the 11th International Congress on the Chemistry of Cement, Durban, South Africa, 11–16 May 2003; Volume 16802, pp. 1248–1259.
51. *IS:2541-1991*; Preparation and Use of Lime Concrete. Bureau of Indian Standards: Delhi, India, 1991.
52. *IS:2542*; (Part 1) Methods of Test for Gypsum Plaster, Concrete and Products. Bureau of Indian Standards: Delhi, India, 1978.
53. Narayanan, N.; Ramamurthy, K. Structure and properties of aerated concrete: A review. *Cem. Concr. Compos.* **2000**, *22*, 321–329. [CrossRef]
54. *IS:12089-1987*; Specification for Granulated Slag for the Manufacture of Portland Slag Cement. Bureau of Indian Standards: Delhi, India, 1987; pp. 1–14.
55. *IS 456*; Concrete, Plain and Reinforced. Bureau of Indian Standards: Delhi, India, 2000; pp. 1–114.
56. Dvorkin, L.; Lushnikova, N.; Sonebi, M. Application areas of phosphogypsum in production of mineral binders and composites based on them: A review of research results. *MATEC Web Conf.* **2018**, *149*, 01012. [CrossRef]
57. *BIS:3812*; (Part 1) Indian Standard Pulverized Fuel Ash-Specification (Second Revision). Bureau of Indian Standards: Delhi, India, 2003.

58. *IS:2185*; Indian Standard Concrete Masonry Units, Part 1: Hollow and Solid Concrete Blocks. Bureau of Indian Standards: Delhi, India, 2005; p. 17.
59. RILEM Technical Committee. Modulus of rupture of autoclaved aerated concrete/Résistance à la flexion du béton cellulaire autoclavé. *Mater. Struct.* **1985**, *18*, 402–405. [CrossRef]
60. Bonakdar, A.; Babbitt, F.; Mobasher, B. Physical and mechanical characterization of fiber-reinforced aerated concrete (FRAC). *Cem. Concr. Compos.* **2013**, *38*, 82–91. [CrossRef]